# Folding Points to a Point and Lines to a Line

Hugo A. Akitaya\* Brad Ballinger<sup>†</sup> Erik D. Demaine<sup>‡</sup> Thomas C. Hull<sup>§</sup> Christiane Schmidt<sup>¶</sup>

### **Abstract**

We introduce basic, but heretofore generally unexplored, problems in computational origami that are similar in style to classic problems from discrete and computational geometry.

We consider the problems of folding each corner of a polygon P to a point p and folding each edge of a polygon P onto a line segment  $\ell$  that connects two boundary points of P and compute the number of edges of the polygon containing p or  $\ell$  limited by crease lines and boundary edges.

#### 1 Introduction

Many classic problems from discrete and computational geometry that concern simple statements about points and lines in the plane, such as, "Given n points in the plane, how do we determine their convex hull?" or "Into how many regions do n lines in general position divide the plane?" Similarly basic questions can be asked about origami, but none seem to have been fully explored in the literature. In this paper we investigate two such questions in computational origami. Both involve starting with a convex-polygon piece of paper P.

- 1. Fold and unfold each corner of P, in turn, to a chosen point  $p \in P$  so that p will be contained in a polygon  $Q_p$  whose interior is uncreased and sides are either the crease lines or the boundary edges of P; see Figure 1(a). How many sides can  $Q_p$  have?
- 2. Let  $a,b \in \partial P$  (the boundary of P), and let  $\ell'$  be the line that contains the line segment  $\ell = \overline{ab}$ . Fold each side of P onto  $\ell'$ , and let  $Q_{\ell}$  be the polygon limited by the crease lines that contains  $\ell$ ; see Figure 1(b). How many sides can  $Q_{\ell}$  have?

In these problems the point p and line  $\ell$  may be chosen to lie on the boundary of P. Our aim is to find straightforward methods for calculating  $|Q_p|$  and  $|Q_\ell|$  so as to

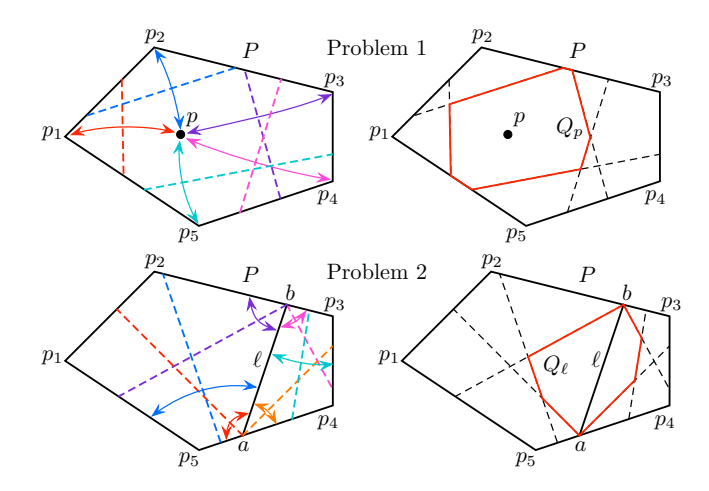


Figure 1: Illustrations of Problems 1 and 2.

create visualizations for which choices of p and  $\ell$  will give us different answers.

Problem 1 was first investigated by Kazuo Haga [6, 7, 8], but only in the case where P is a square. We will see that the full version of Problem 1, including the case where P is the whole plane, is a natural application of Voronoi diagrams and Delaunay triangulations. Problem 2 is solved using event circles of the straight skeleton of P.

## 2 Folding Points to a Point

To first simplify Problem 1, let  $S = \{p_1, \ldots, p_n\}$  be the vertices of the polygon P and let us, for now, ignore the sides of P, focusing on only folding an arbitrarily-chosen point p to the points in S; call this *Problem 1a*. We introduce notation for Voronoi diagrams (see [2, 4]). Given  $a, b \in \mathbb{R}^2$ , define the halfplane determined by a and b that contains a to be

$$h(a,b) = \{x \in \mathbb{R}^2 \mid ||x - a|| \le ||x - b||\},\$$

where ||.|| denotes Euclidean norm. The *Voronoi region* Vor(p, A) containing point p relative to a finite point set A is defined as

$$\operatorname{Vor}(p,A) = \{x \in \mathbb{R}^2 \mid ||x-p|| \leq ||x-a|| \text{ for all } a \in A\}.$$

A standard result (see [4, Theorem 4.1]) is that Vor(p, A) is equal to the intersection of halfplanes determined by p and the points in A:

<sup>\*</sup>Department of Computer Science, University of Massachusetts Lowell, hugo\_akitaya@uml.edu

<sup>†</sup>Humbolt State University, bradley.ballinger@humboldt.edu ‡Computer Science and Artificial Intelligence Laboratory,

<sup>&</sup>lt;sup>†</sup>Computer Science and Artificial Intelligence Laboratory, Massachusetts Institute of Technology, edemaine@mit.edu

 $<sup>\</sup>S{Department}$  of Mathematics, Western New England University, thull@wne.edu

<sup>¶</sup>Communications and Transport Systems, ITN, Linköping University, christiane.schmidt@liu.se

#### Theorem 1

$$\operatorname{Vor}(p,A) = \bigcap_{a \in A} h(p,a).$$

The *Voronoi diagram* for a finite point set  $S = \{p_1, \ldots, p_n\}$  is then the collection of Voronoi regions  $Vor(p_i, S \setminus \{p_i\})$  for  $i = 1, \ldots, n$ .

**Theorem 2** Let  $Q_p$  be the polygon containing p limited by the crease lines made from folding p to each point in S. Then  $Q_p = Vor(p, S)$ .

**Proof.** This follows almost immediately from the fact that when we fold a point  $p_i \in S$  to the point p, the crease line L that is made is the perpendicular bisector of the segment joining  $p_i$  and p. But L is also the boundary of the halfplane  $h(p, p_i)$ , and  $Q_p$  will be contained in all such halfplanes. Furthermore, any point that is contained in all the halfplanes  $h(p, p_i)$  will, by definition, also be in  $Q_p$ . This proves the result.

This connection between origami and Vonoroi diagrams is known to origami artists. In fact, one of the easiest ways to construct a Voronoi diagram is to draw the point set S on a piece of paper and carefully fold pairs of points in S together, creasing the various halfplane boundaries. See [11] for more details.

We let  $\operatorname{conv}(S)$  denote the convex hull of the set S. The definition of Voronoi region implies that  $\operatorname{Vor}(p,S)$  will be unbounded if p is not in the interior of  $\operatorname{conv}(S)$ . Thus Theorem 2 implies the following:

Corollary 3 If  $p \notin \operatorname{int}(\operatorname{conv}(S))$ , then  $Q_p$  is unbounded.

Now let Del(S) denote the Delaunay triangulation of a finite point set S. For details on Del(S), see [2, 4]; we remind the reader of three key properties of Del(S):

- 1. The interior of the circumcircle of any triangle in Del(S) contains no points of S.
- 2. If there exists a circle containing two points  $p_1, p_2 \in S$  whose interior contains no points of S, then  $p_1p_2$  is an edge of Del(S).
- 3. Del(S) is the planar dual graph of the Voronoi diagram graph of S (i.e., the dual of the planar graph obtained by the boundaries of the Voronoi regions and ignoring the outside region of this graph).

Property 3 gives us a solution to Problem 1a. Let  $|Q_p|$  denote the number of sides of the polygon  $Q_p$ .

**Theorem 4** Given a finite point set  $S \subset \mathbb{R}^2$  and a point p, a solution to Problem 1a is  $|Q_p| = \deg(p)$ , the degree (i.e., valency) of p in  $\mathrm{Del}(S \cup \{p\})$ .

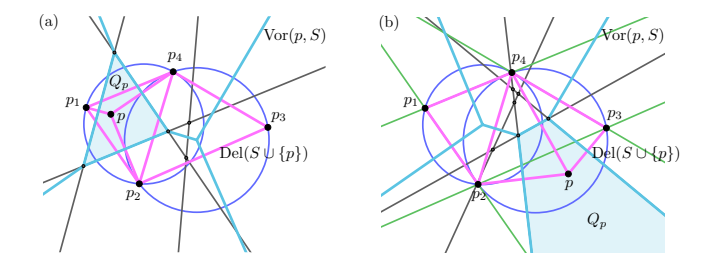


Figure 2: The region  $Q_p$  for a point set  $S = \{p_1, \ldots, p_4\}$  where (a)  $p \in \text{conv}(S)$  and (b)  $p \notin \text{conv}(S)$ . Black lines are the creases made when folding p to points in S. Circles are the circumcircles of the triangles in Del(S). Green lines are supporting hyperplanes of conv(S).

See Figure 2 for illustrations of this Theorem.

A more complete solution to Problem 1a would be to partition the plane into regions of constant  $|Q_p|$ . Since computing  $\mathrm{Del}(S \cup \{p\})$  for many choices of p is cumbersome, we seek a more computationally direct way of solving Problem 1a. For example, an algorithm that relies only on  $\mathrm{Del}(S)$  instead of  $\mathrm{Del}(S \cup \{p\})$  would be preferable. We achieve this via a sequence of Lemmas which, while tailored to our specific problem, follow from basic facts about Delaunay triangulations and Voronoi diagrams (see [2, 4]).

For  $x \in \mathbb{R}^2$ , let us define  $T_S(x)$  as the set of triangles in  $\mathrm{Del}(S)$  whose circumcircles contain x in their interior.

**Lemma 5** If  $p_i \in S$  is in the interior of conv(S), the edge  $pp_i$  is in  $Del(S \cup \{p\})$  if and only if  $T_S(p)$  contains a triangle that has  $p_i$  as a corner.

**Proof.** First assume that  $pp_i$  is in  $Del(S \cup \{p\})$ . The edge must be part of at least one triangle  $p_ip_jp$ . Then, by property 1, there is an interior-empty circle containing p,  $p_i$  and  $p_j$ . Ignoring p for the moment, grow this circle maintaining  $p_ip_j$  as a chord and so that p remains inside this circle until the circle contains another point in S; this must happen because  $p_ip_j$  is not in the boundary of conv(S). The obtained circle then contains three points in S and its interior contains only p, by construction. The triangle defined by the points on this circle is in  $T_S(p)$ .

Now assume that a triangle  $T \in T_S(p)$  has  $p_i$  as a corner. By property 1, there is a circle C containing  $p_i$  whose interior contain only p and no other point. We shrink C along its diameter that contains  $p_i$ , anchored at  $p_i$  until we obtain a circle C' containing p. By construction, the interior of C' is empty. By property 2,  $pp_i$  is an edge in  $Del(S \cup \{p\})$ .

**Lemma 6** Let  $T_S(p) = \{T_1, \ldots, T_k\}$  and G be the graph whose vertex set is  $T_S(p)$ , and with an edge  $T_iT_j$  if  $T_i$  and  $T_j$  share a side. So long as  $p \notin S$ , then G is a tree.

**Proof.** We first claim that a triangle T in  $Del(S \cup \{p\})$  that does not have p as a corner is also in Del(S). By property 1, the interior of the circumcircle of T is empty and deleting p does not change that. Hence, T is also in Del(S) as claimed.

If we delete p from  $\text{Del}(S \cup \{p\})$  (and all edges adjacent to p) we either get a single polygonal star-shaped hole or a pocket polygon (a cavity on the boundary of conv(S)). Since  $p \notin S$ , in order to obtain Del(S) we can simply triangulate the hole or pocket by the above claim. By Lemma 5, the new triangles are exactly  $T_S(p)$ . The dual graph of a triangulation of a simple polygon is a tree.

**Lemma 7** If  $p \in \text{conv}(S)$  and  $p \notin S$ , then  $|Q_p| = |T_S(p)| + 2$ .

**Proof.** Let  $T_S(p) = \{T_1, \ldots, T_k\}$ . One of these triangles, say  $T_a$ , contains p because  $p \in \operatorname{conv}(S)$ . By Theorem 4,  $|Q_p| = \deg(p)$  in  $\operatorname{Del}(S \cup \{p\})$ , which equals the number of distinct vertices among the triangles  $T_1, \ldots, T_k$ , by Lemma 5. By Lemma 6, the edge-adjacency graph of  $T_S(p)$  is a tree, which we can root at  $T_a$ . If we first count the three vertices in  $T_a$ , then we traverse the tree and for each additional triangle that we discover in the traversal we add only one vertex to our count. This gives us k+2 distinct vertices among the triangles in  $T_S(p)$ , and so  $\deg(p) = k+2$ , as claimed.  $\square$ 

Note that Lemma 7 allows p to be on the boundary of conv(S) (but not in S), in which case  $Q_p$  will be unbounded. In fact, for some areas nearby but outside conv(S), Lemma 7 will still apply. But to handle any choice of  $p \in \mathbb{R}^2$ , we need to consider certain supporting halfplanes of conv(S).

The boundary of conv(S) is a polygon; denote its vertices by  $q_1, \ldots, q_m$ . Let  $H(q_i, q_{i+1})$  denote the supporting halfplane of conv(S) that contains the segment  $q_iq_{i+1}$  on its boundary, and assume that the indices are cyclic so that this notation includes  $H(q_m, q_1)$ .

Let  $\overline{H}(p)$  denote the number of halfplanes  $H(q_i, q_{i+1})$  that do not contain the point p.

**Lemma 8** If  $p \notin \text{conv}(S)$  or  $p \in S$  then  $|Q_p| = \overline{H}(p) + |T_S(p)| + 1$ .

**Proof.** Suppose p is far enough away from  $\operatorname{conv}(S)$  so that none of the circumcircles of the triangles in  $\operatorname{Del}(S)$  contain it. If  $H(q_i, q_{i+1})$  does not contain p, then p will be able to "see" both  $q_i$  and  $q_{i+1}$ . That is, a straight line segment from p to either  $q_i$  or  $q_{i+1}$  will not intersect  $\operatorname{conv}(S)$ . Thus, in  $\operatorname{Del}(S \cup \{p\})$ , p will be adjacent to  $q_i$  and  $q_{i+1}$ . For all supporting halfplanes that do not contain p, their corresponding vertices  $q_i$  will form a path on the boundary of  $\operatorname{conv}(S)$ , and we have that  $\operatorname{deg}(p) = \overline{H}(p) + 1$ .

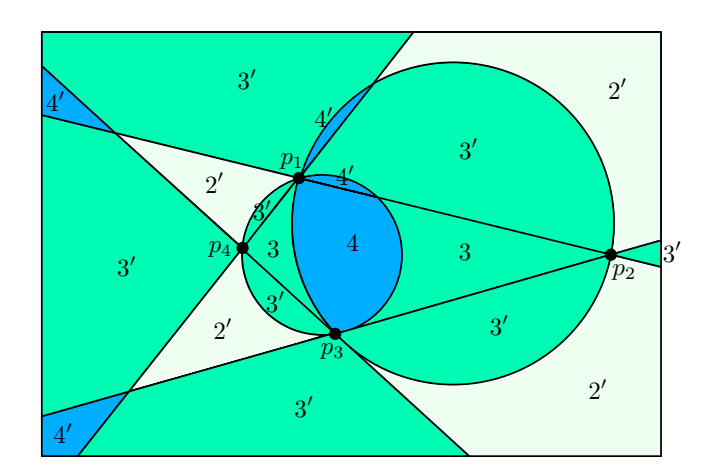


Figure 3: The plane partitioned into regions of constant  $|Q_p|$  for a point set  $S = \{p_1, \ldots, p_4\}$  in Problem 1a. Numbers marked with a prime symbol indicate regions where p gives an unbounded set  $Q_p$ .

If p is also in a circumcircle of a triangle T in Del(S) (an example of this is shown in Figure 2(b)), then by Lemma 5, p will be connected with new edges to every corner of T. Similar to the proof of Lemma 7, we can use Lemma 6 to show that there are  $|T_S(p)| + 2$  such edges. However, two of these edges are double counted because two endpoints are on the boundary of conv(S). Thus the "+2" in Lemma 7 is not needed, and we arrive at  $|Q_p| = \overline{H}(p) + |T_S(p)| + 1$ .

If  $p \in S$  then p is contained in all of the supporting halfplanes of  $\operatorname{conv}(S)$ . In fact, the situation is like that of Lemma 7 and its proof, except that  $Q_p$  will be unbounded and have one less side than the cases of Lemma 7 since we cannot fold p to itself. Thus  $|Q_p| = |T_S(p)| + 1$  and we are done.

When  $p \in \text{conv}(S)$ , we have that  $\overline{H}(p) = 0$ , so we can combine Lemmas 7 and 8 if we add an indicator function I(p) which equals 1 if  $p \in (\text{conv}(S) \setminus S)$  and 0 otherwise.

**Theorem 9** Using the notation of Problem 1a, we have

$$|Q_p| = \overline{H}(p) + |T_S(p)| + I(p) + 1.$$

Figure 3 illustrates how Theorem 9 can be used to partition the plane into regions of constant  $|Q_p|$ .

**Remark on general position:** Notice that no requirement has been made for the points in S to be in general position (no three points on a line). This is because no such requirement is necessary, but some care must be taken. If three points  $p_1, p_2, p_3 \in S$  lie on a line, then those points cannot make a triangle in Del(S), and neither can they make a circumcircle. However, if these three collinear points lie on the boundary of conv(S),

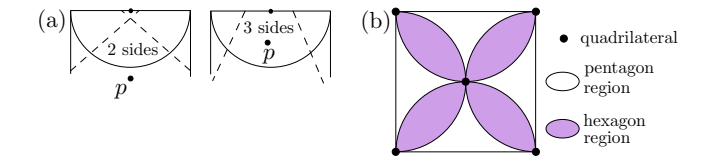


Figure 4: (a) Folding two corners to p with p outside, then inside, the side's midpoint circle. (b) The full solution to Problem 1 on a square.

say in order  $p_1$ ,  $p_2$ , then  $p_3$ , then they will form two supporting halfplanes, one for the segment  $p_1p_2$  and one for  $p_2p_3$ . This will affect the count of  $\overline{H}(p)$ ; if p is not in the halfplane  $H(p_1, p_2)$  then it will also not be in  $H(p_2, p_3)$ , and so the side of  $\operatorname{conv}(S)$  made by  $p_1$ ,  $p_2$ , and  $p_3$  will "count twice" in  $\overline{H}(p)$  if p is on the other side of it.

Remark on computation time: The Voronoi diagram can be computed in  $O(n \log n)$  time [5] and, thus, we can compute  $Q_p$  in the same asymptotic time. Note that  $Q_p$  may have  $\Omega(n)$  sides and that the boundary of  $Q_p$ encodes the sorted cyclic order of the points adjacent to p in  $Del(S \cup \{p\})$ . Then, this is the best possible bound in the decision tree computation model. By Theorem 9, the partition of the plane into regions of constant  $|Q_n|$ is given by an arrangement of circles and lines. Note that such arrangement can be of size  $\Theta(n^2)$ . Since each pair of these curves can only intersect at most twice, a sweep line algorithm can compute the arrangement in  $O(n^2 \log n)$  time. Then, with  $O(n^2 \log n)$  preprocessing time, given a query point p, Problem 1a can be solved in  $O(\log n)$  time using a point-location data structure such as Kirkpatrick's [10].

#### 3 Folding Corners of a Polygon to a Point

We return to Problem 1, folding the corners of a polygon P to a point p, so that the sides of  $Q_p$  may now be crease lines or edges of P.

As Haga discusses in his solution of the case where P is a square [6], the key is to see how close p needs to be to a boundary side of the paper in order to make that boundary add a side to  $Q_p$ . Imagine a semicircle C drawn on the paper whose center is the midpoint of a boundary side of P and with diameter equal to the length of that side. Then the endpoints of C equal two corners of P. If p is inside C, then when these two corners are folded to p their creases will not intersect at a point inside P, making the boundary edge between them add a side to  $Q_p$ . But if p lies on C or outside of C, then the two crease lines will intersect on P's boundary or inside it, respectively, implying that the boundary side in question will not contribute a side to  $Q_p$ . See Figure 4(a) for an illustration of this in the case where P is a square.

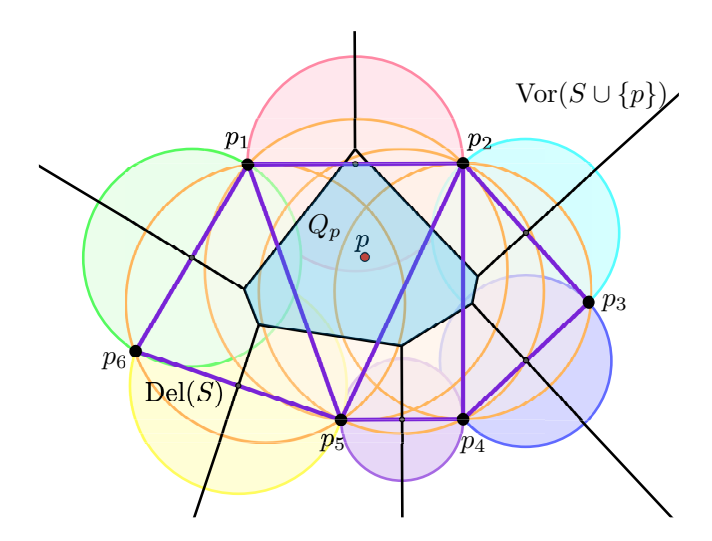


Figure 5: A generalized Problem 1 example on an irregular hexagon-shaped piece of paper  $S = \{p_1, \ldots, p_6\}$ . p is located in four circumcircles of Del(S) and one midpoint circle, giving us  $|Q_p| = 7$ .

Thus, Haga's original solution is to draw four semicircles on our square, each centered at a different midpoint of the sides and with diameter equal to that side. We may then determine  $|Q_p|$  by counting how many of the semicircle interiors contain p. If p is in the interior of only one semicircle, then only one boundary edge will contribute a side to  $Q_p$ , giving us  $|Q_p| = 5$ . If p is in two semicircle interiors, then two boundary sides will contribute, giving  $|Q_p| = 6$ . As can be seen in Figure 4(b), p can be in at most two of these semicircle interiors, so this solves the problem and gives us a partition of the square into regions of constant  $|Q_p|$ .

What Haga's original problem solution hides is the influence of Voronoi diagrams and Delaunay triangulations, because in the case where our paper is a square, the circumcircles of  $\mathrm{Del}(S)$  are equal and merely circumscribe the square. Thus, in our full Problem 1 statement we can combine our result from Problem 1a to obtain a full solution.

Let M(p) denote the number of *midpoint circles* (circles centered at a midpoint of the polygon-shaped paper's edge and with diameter equal to that edge length) that contain p in their interior.

**Theorem 10** Given a convex polygon of paper P and a point  $p \in P$ , we have  $|Q_p| = M(p) + |T_S(p)| + 2$ .

An illustration of this solution to Problem 1 is shown in Figure 5.

### 4 Folding Lines to a Line

To recap Problem 2, we take two points a, b on the boundary of a convex polygon P, let  $\ell'$  be the line containing the segment  $\ell = \overline{ab}$ , and then fold and unfold

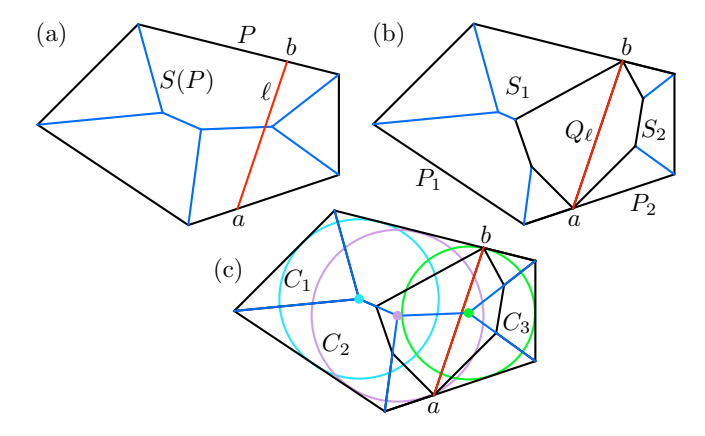


Figure 6: Analyzing Problem 2. (a) The polygon P, line  $\ell$ , and the straight skeleton/medial axis S(P). (b) The skeletons  $S_1, S_2$  and the polygon  $Q_{\ell}$  containing  $\ell$ . (c) The event circles  $C_1$ ,  $C_2$ , and  $C_3$  of S(P); here two of them intersect  $\ell$ .

each side of P onto  $\ell'$  in turn. We wish to describe the number of sides of the polygon  $Q_{\ell}$  that contains  $\ell$  and is limited by the crease lines we made. Let V(P) and E(P) denote the vertex and edge sets of P.

While Problem 1 was determined by the Voronoi diagram of V(P), Problem 2 is governed by the straight skeleton (or medial axis, as these are equivalent on convex polygons) of E(P). Towards that end, we will establish some notation, based on that of [1]. Let S(P) denote the straight skeleton/medial axis of P, which we may think of the set of points x inside (or on the boundary) of P such that x is equidistant between at least two points of  $\partial P$ . Since P is convex, S(P) will be a straight-line graph drawn on P that will include segments bisecting the angles of P (see Figure 6(a)).

The non-leaf vertices of S(P) are called *event points* and the circles centered at these points that are tangent to their nearest sides of P are called the *event circles* of S(P). Label these event circles  $C_1, \ldots, C_k$  and let  $\mathcal{C}^{\ell}$  be the subset of these circles that intersect  $\ell$  (see Figure 6(c)).

Since  $\ell$  splits P into two polygons,  $P_1$  and  $P_2$ , we may find their straight skeletons as well; call them  $S_1$  and  $S_2$  respectively (see Figure 6(b)). One of each pair will be degenerate if a and b are on the same edge of P.

We define  $b(e,\ell)$  to be the angle bisector between the line containing the edge  $e \in E(P)$  and  $\ell'$  (or, if these lines are parallel, let  $b(e,\ell)$  be the line that is equidistant between these lines). Let  $h(\ell,e)$  and  $h(e,\ell)$  be the halfplane induced by  $b(e,\ell)$  that contains  $\ell$  and e, respectively.

# Lemma 11 $V(Q_{\ell}) \setminus \{a, b\} \subset S(P)$ .

**Proof.** We create the sides of  $Q_{\ell}$  by folding a side  $e \in E(P)$  to  $\ell$ , making a crease that is a segment along the

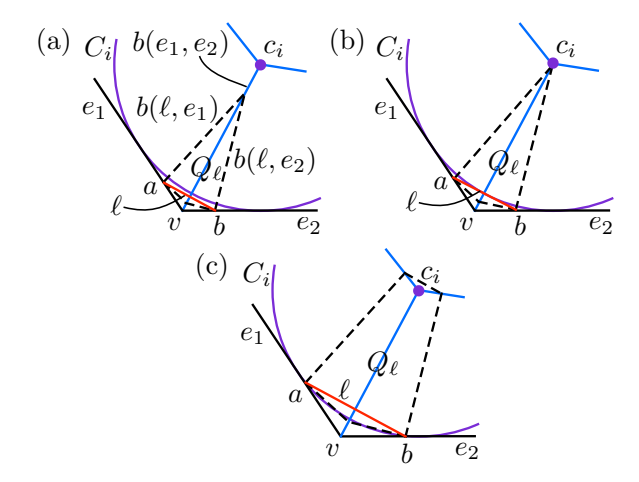


Figure 7: For Theorem 14's proof. (a) For  $\ell$  close enough to a vertex  $v \in V(P)$ ,  $Q_{\ell}$  will be a quadrilateral. (b) If  $\ell$  is tangent to the event circle  $C_i$  closest to v,  $Q_{\ell}$  remains a quadrilateral, but critically. (c) When  $\ell$  intersects the interior of  $C_i$ , a side is added to  $Q_{\ell}$ .

bisector  $b(e, \ell)$ . Thus the sides of  $Q_{\ell}$  will lie along the edges of the skeletons  $S_1$  and  $S_2$ , and the vertices of  $Q_{\ell}$  (aside from a and b) will be event points of  $S_1$  and  $S_2$ , which must lie on S(P).

**Lemma 12** Let  $C_{\ell}(q)$  be the circle centered at q that is tangent to  $\ell$ . Then  $q \in \text{int}(Q_{\ell})$  if and only if  $e \cap C_{\ell}(q) = \emptyset$  for all  $e \in E(P)$ .

**Proof.** Let  $q \in \operatorname{int}(Q_{\ell})$  and consider any edge  $e \in E(P)$ . Then  $q \in h(\ell, e)$  and, hence,  $e \cap C_{\ell}(q) = \emptyset$ .

Consider  $q \notin \operatorname{int}(Q_{\ell})$ . Then there exists an edge  $e \in E(P)$  with  $q \in h(e, \ell)$ , whereby  $e \cap C_{\ell}(q) \neq \emptyset$ .

**Lemma 13** Let C be an event circle of S(P) that does not intersect  $\ell$ . Then the center of C will not be a vertex of  $Q_{\ell}$ .

**Proof.** Clearly the center of such a circle C cannot be a or b. Any other vertex of  $Q_{\ell}$  lies on S(P) by Lemma 11 as well as on either  $S_1$  or  $S_2$ . Thus if C were centered at a point in  $V(Q_{\ell}) \setminus \{a, b\}$  then C would be tangent to  $\ell$ , which we forbid in this Lemma.

As our solution to Problem 2, we claim that the number of sides of  $Q_{\ell}$  will equal the number of event circles that intersect  $\ell$  plus four, unless one or more of  $\{a,b\}$  are also vertices of P, in which case those points must be subtracted.

**Theorem 14**  $|V(Q_{\ell})| = |\mathcal{C}^{\ell}| + 4 - |\{x \in \{a, b\} : x \in V(P)\}|.$ 

**Proof.** We let  $\ell$  sweep over P, starting at a vertex  $v \in V(P)$  that is adjacent to sides  $e_1, e_2 \in E(P)$ . The bisector  $b(e_1, e_2)$  at v will lie along the edge  $\overline{vc_i}$  of the

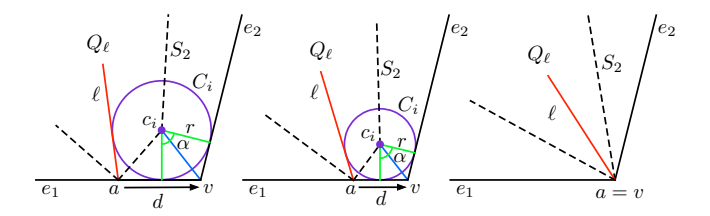


Figure 8: Showing, for the proof of Theorem 14, how if an endpoint a of  $\ell$  equals a vertex v of P, then  $Q_{\ell}$  will lose a side.

straight skeleton S(P) at v, where  $c_i$  is the center of an event circle  $C_i$  that is tangent to the sides  $e_1$  and  $e_2$ . Now, if  $\ell$  is drawn close enough to v so that  $\ell$  lies outside or tangent to  $C_i$ , then  $Q_{\ell}$  will be a quadrilateral. This is because if  $\ell$  is outside of  $C_i$  then the bisectors  $b(\ell, e_1)$  and  $b(\ell, e_2)$  will intersect on S(P) between v and  $c_i$ , and if  $\ell$  is tangent to  $C_i$  this intersection will occur at  $c_i$ , as we have  $c_i \notin Q_{\ell}$  by Lemma 12. See Figures 7(a) and (b).

If, however, we sweep  $\ell$  so that it intersects the interior of  $C_i$ , then the bisectors  $b(\ell, e_1)$  and  $b(\ell, e_2)$  will intersect along  $b(e_1, e_2)$  beyond the point  $c_i$ , meaning that they will cross other segments of S(P) before such an intersection. By Lemma 11, in order for the vertices of  $Q_{\ell}$  to remain on S(P) we must have that a side was added to  $Q_{\ell}$ , as demonstrated in Figure 7(c).

We then sweep  $\ell$ , continuously moving a and b clockwise and counterclockwise, respectively, from v along  $\partial P$ . When  $\ell$  intersects the interior of an event circle  $C_i$  in S(P), thus adding a circle to  $\mathcal{C}^{\ell}$ , an additional side will be added to  $Q_{\ell}$ . All event circles that do not intersect  $\ell$  will not contribute sides to  $Q_{\ell}$  by Lemma 13.

If  $a \in V(P)$  one event circle of either  $S_1$  or  $S_2$  will disappear at this vertex: Let a be close to a vertex  $v \in V(P)$ , say with d(a,v)=d, see Figure 8. We consider the circle  $C_i$  tangent to  $\ell$  and the two edges incident to v,  $e_1$  and  $e_2$ . When we move a towards v, the angle  $\alpha$  between the two radii from the center of  $C_i$  to  $e_1$  and  $e_2$  is constant (since  $c_i$  will move closer to v along the bisector  $b(e_1,e_2)$  segment of S(P) as a approaches v). Hence, the ratio between d and the radius r of  $C_i$  is constant. Consequently, d approaches zero when r goes to zero, and  $C_i$  disappears at the limit. The same holds true for  $b \in V(P)$ .

Remark on computation time: The medial axis of a simple polygon P with n vertices can be computed in O(n) time [3] and, thus, we can compute  $Q_{\ell}$  in the same asymptotic time by computing the medial axis of the two convex polygons obtained by splitting P with  $\ell$ . Note that the complexity of  $Q_{\ell}$  is  $\Omega(n)$  in the worst case and thus this time bound is optimal.

#### 5 Bounds and Visualization for Problem 2

When we follow the computation from Theorem 14 to determine the number of sides/edges of our polygon  $Q_{\ell}$ , we need to compute the event circles of the straight skeleton intersecting the line segment  $\ell$ . In this section, we do not aim for an exact computation of  $|V(Q_{\ell})|$ , instead giving simple bounds.

The line segment  $\ell$  is determined by two points, a, b, on P's boundary. The maximum number of vertices of  $Q_{\ell}$  depends on the location of a and b—we distinguish whether both, one of, or none of a and b are vertices of P:

**Lemma 15** With n = |V(P)|, we have:

- 1. If  $a, b \in \partial P \setminus V(P)$ , then  $|V(Q_{\ell})| \leq n + 2$ .
- 2. If  $a \in V(P)$ ,  $b \in \partial P \setminus V$ , then  $|V(Q_{\ell})| \leq n+1$ .
- 3. If  $a, b \in V(P)$ , then  $|V(Q_{\ell})| \leq n$ .

**Proof.** For the number of event circles  $C_1, \ldots, C_k$  in P (or vertices of S(P)), we have  $|\{C_1, \ldots, C_k\}| = n-2$  (see Aichholzer and Aurenhammer [1]). In  $\mathcal{C}^{\ell}$ , we consider only the subset of these event circles that intersect  $\ell$ , hence,  $|\mathcal{C}^{\ell}| \leq |\{C_1, \ldots, C_k\}| = n-2$ . With  $|\{x \in \{a, b\}: x \in V(P)\}| = 0$  for  $a, b \in \partial P \setminus V(P)$ ,  $|\{x \in \{a, b\}: x \in V(P)\}| = 1$  for  $a \in V(P), b \in \partial P \setminus V(P)$ , and  $|\{x \in \{a, b\}: x \in V(P)\}| = 2$  for  $a, b \in V(P)$ , the claim follows directly from Theorem 14.

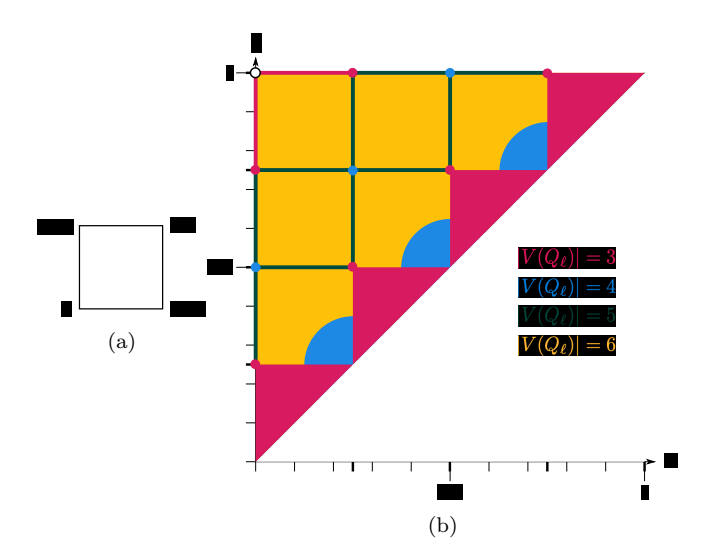


Figure 9: Example for the visualization of the exact value of  $|V(Q_{\ell})|$  for a square: (a) parameterization and (b) configuration space.

**Visualization.** To visualize upper bounds, lower bounds, or the exact value of  $|V(Q_{\ell})|$ , we parameterize  $\partial P$  starting from and ending at an arbitrary vertex

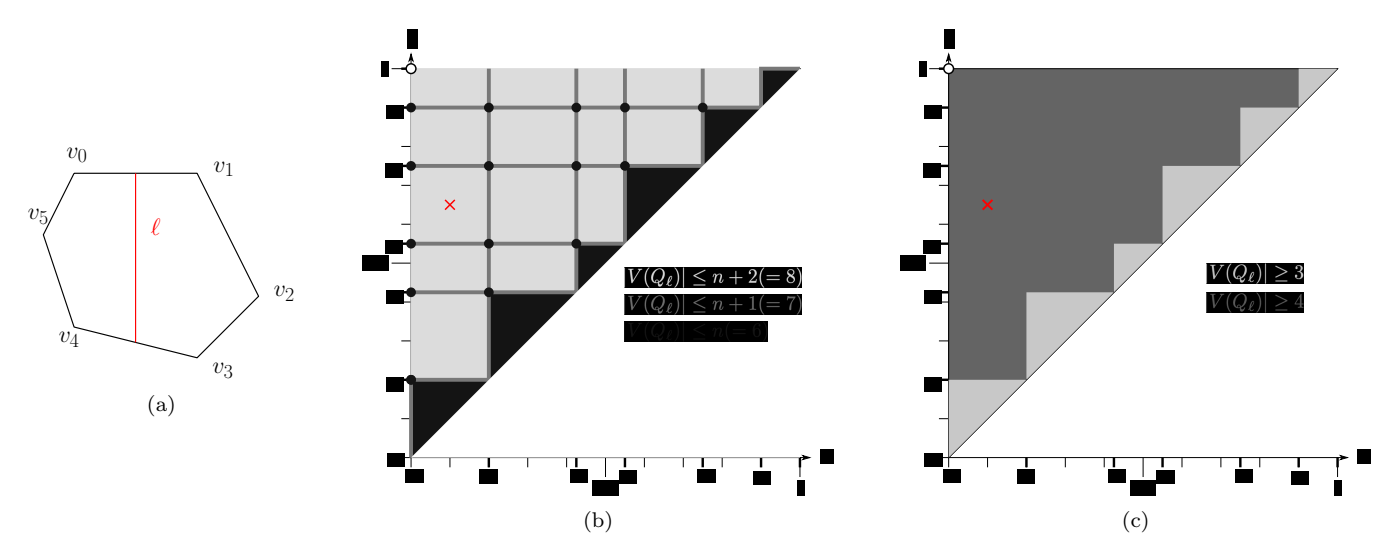


Figure 10: An example of Problem 2 visualization. (a) A 6-gon with a possible line segment  $\ell$  (in red) with  $a, b \in \partial P \setminus V$ . (b) Upper bounds from Lemma 15, (c) lower bounds. The red cross in (b) and (c) represents the line segment  $\ell$  from (a).

 $v \in V(P) = \{v_0, \dots, v_{n-1}\}$  (w.l.o.g., we choose  $v = v_0$ ). We consider a unit square, with the location of a on the x-axis and the location of b on the y-axis. We color all points of the triangle above the line segment  $\overline{(0,0)}, \overline{(1,1)}$  according to the valid upper bound, lower bound, or the value of  $|V(Q_\ell)|$ . For an example with exact values of  $|V(Q_\ell)|$  when P is a square see Figure 9, for an example of upper and lower bounds when P is a 6-gon see Figure 10.

#### 6 Conclusion

The problems presented here are fairly abstract and seem divorced from computational origami problems that have been previously studied. Connections may exist, however. For example, the straight skeleton is useful in algorithms for origami design [12], and so the line  $\ell$  in Problem 2 could be interpreted as separating our polygon P of paper into two regions, each of which could then be folded into different origami bases via their straight skeletons.  $Q_{\ell}$  would then represent the polygon of paper that, when folded along  $\ell$ , links the two bases together. Knowing  $|Q_{\ell}|$  in advance might help the origami designer plan how to sink the flaps of paper adjoining  $Q_{\ell}$ , a step that is often useful when turning an algorithmicly-designed origami base into a representational model.

At first glance, one might think that Problems 1 and 2 would be duals to each other in the projective geometry sense, since the first concerns folding points to points and the second lines to lines. However, this is incorrect, mainly because the operation of folding a point  $p_1$  to another point  $p_2$ , which makes a crease line that is the perpendicular bisector of  $\overline{p_1p_2}$ , is not dual to the operation of folding a line  $l_1$  to  $l_2$ , which forms the bisector of

 $l_1$  and  $l_2$ . This is why our solutions to these two problems, while similar in flavor, are not reducible from one another.

We hope that this work will inspire others to consider similar folding problems in computational origami. Indeed, the list of basic origami operations (see [9, Chapter 1]) would be a good place to start to investigate what other simple folding problems are possible. Also, the work of Kazuo Haga, which is characterized by playful investigations of simple folds (what he calls *origamics*) led directly to our investigations in the present paper. Haga's work, in particular [7], certainly contains avenues for further study.

## Acknowledgments

This work was conducted at the 2018 and 2019 Bellairs Workshops on Computational Geometry, co-organized by Erik Demaine and Godfried Toussaint. We thank the other participants of the workshop for helpful discussions, especially Klara Mundilova and Tomohiro Tachi. H. A. A. was partially supported by NSF grants CCF-1422311, CCF-1423615. T. C. H. was partially supported by NSF grant DMS-1906202 and C. S. was partially supported by Jubileumsanslaget från Knut och Alice Wallenbergs Stiftelse and Vinnova grant 2018-04101.

### References

[1] O. Aichholzer and F. Aurenhammer, Straight Skeletons for General Polygonal Figures in the Plane, Proc. 2nd Ann. Int'l. Computing and Combinatorics Conf. CO-COON'96, Lecture Notes in Computer Science, volume 1090, pages 117-126, Hong Kong, 1996. Springer Verlag.

- [2] F. Aurenhammer, R. Klein, and D. Lee, Voronoi Diagrams and Delaunay Triangulations, World Scientific, Singapore, 2013.
- [3] F. Chin, J. Snoeyink, and C. A. Wang, Finding the medial axis of a simple polygon in linear time, *Discrete* & Computational Geometry, 1999, 21(3), 405–20.
- [4] S. Devadoss and J. O'Rourke, Discrete and Computational Geometry, Princeton University Press, Princeton, NJ, 2011.
- [5] S. Fortune, A sweepline algorithm for Voronoi diagrams, Algorithmica, 1987, 2(1), 153–174.
- [6] K. Haga, Proposal of a term origamics for plastic origami-workless scientific origami, in Second International Meeting of Origami Science and Scientific Origami Abstracts, Seian University of Art and Design, Otsu, Japan, 1994, 29–30.
- [7] K. Haga, Origamics: Mathematical Explorations Through Paper Folding, World Scientific Publishing Co., River Edge, NJ, 2008.
- [8] T. Hull, Project Origami: Activities for Exploring Mathematics, 2nd ed., CRC Press/A K Peters, Boca Raton, FL, 2012.
- [9] T. Hull, Origametry: Mathematical Methods in Paper Folding, Cambridge University Press, Cambridge, UK, 2020.
- [10] D. Kirkpatrick, Optimal search in planar subdivisions, SIAM Journal on Computing, 1983, 12(1), 28–35.
- [11] R. Kraft, Orthoginal Voronoi molecules, in Lang et al. ed., Origami<sup>7</sup>: The Proceedings from the 7th International Meeting on Origami in Science, Mathematics, and Education, Tarquin, St. Albans, UK, 2018, 607– 621.
- [12] R. J. Lang, A computational algorithm for origami design, in *Proceedings of the Twelfth Annual Symposium on Computational Geometry*, ACM, 1996, 98–105.